The optical cell rotator

Moritz K. Kreysing[1,2], Tobias Kießling[1], Anatol Fritsch[1], Christian Dietrich[3], Jochen R. Guck[1,2] and Josef A. Käs[1]

[1] *Department for Experimental Physics I, University of Leipzig, Leipzig, Germany*
[2] *Cavendish Laboratory, Department of Physics, University of Cambridge, Cambridge, UK*
[3] *Carl Zeiss MicroImaging GmbH, Jena, Germany*

mkk26@cam.ac.uk

Abstract: The optical cell rotator (OCR) is a modified dual-beam laser trap for the holding and controlled rotation of suspended dielectric microparticles, such as cells. In contrast to optical tweezers, OCR uses two counter-propagating divergent laser beams, which are shaped and delivered by optical fibers. The rotation of a trapped specimen is carried out by the rotation of a dual-mode fiber, emitting an asymmetric laser beam. Experiments were performed on human erythrocytes, promyelocytic leukemia cells (HL60), and cell clusters (MCF-7). Since OCR permits the rotation of cells around an axis perpendicular to the optical axis of any microscope and is fully decoupled from imaging optics, it could be a suitable and expedient tool for tomographic microscopy.

OCIS codes: (140.7010) Laser trapping; (350.4855) Optical tweezers or optical manipulation; (060.2310) Fiber optics; (140.3300) Laser beam shaping; (170.6900) Three-dimensional microscopy; (170.1530) Cell analysis

References and links

1. A. Ashkin, "Acceleration and Trapping of Particles by Radiation Pressure," Phys. Rev. Lett. **24**, 156–159 (1970). http://prola.aps.org/abstract/PRL/v24/i4/p156_1.
2. H. Zhang, and K. Liu, "Optical tweezers for single cells," J. R. Soc. Interface **5**, 671–690 (2008). http://journals.royalsociety.org/index/9804324253112122.pdf.
3. K. Dholakia, and P. Reece, "Optical manipulation takes hold," Nano Today **1**, 18–27 (2006). http://dx.doi.org/10.1016/S1748-0132(06)70019-6.
4. R. A. Beth, "Mechanical Detection and Measurement of the Angular Momentum of Light," Phys. Rev. **50**, 115–125 (1936). http://prola.aps.org/abstract/PR/v50/i2/p115_1.
5. M. E. J. Friese, T. A. Nieminen, N. R. Heckenberg, and H. Rubinsztein-Dunlop, "Optical alignment and spinning of laser-trapped microscopic particles," Nature **394**, 348 (1998). http://arxiv.org/abs/physics/0308113.
6. H. He, M. E. J. Friese, N. R. Heckenberg, and H. Rubinsztein-Dunlop, "Direct Observation of Transfer of Angular Momentum to Absorptive Particles from a Laser Beam with a Phase Singularity," Phys. Rev. Lett. **75**, 826–829 (1995). http://prola.aps.org/abstract/PRL/v75/i5/p826_1.
7. L. Allen, S. M. Barnett, and M. J. Padgett, *Optical Angular Momentum*, (Institute of Physics Publishing, Bristol, 2003). http://stacks.iop.org/1464-4266/6/365.
8. S. Sato, M. Ishigure, and H. Inaba, "Optical trapping and rotational manipulation of microscopic particles and biological cells using higher-order mode Nd: YAG laserbeams," Electron. Lett. **27**, 1831–1832 (1991).
9. R. Dasgupta, S. Mohanty, and P. Gupta, "Controlled rotation of biological microscopic objects using optical line tweezers," Biotechnol. Lett. **25**, 1625–1628 (2003). http://www.springerlink.com/index/T20RW4Q4J7587VX1.pdf.
10. A. O'Neil and M. Padgett, "Rotational control within optical tweezers by use of a rotating aperture," Opt. Lett. **27**, 743–745 (2002). http://ol.osa.org/abstract.cfm?URI=ol-27-9-743.
11. L. Paterson, M. P. MacDonald, J. Arlt, W. Sibbett, P. E. Bryant, and K. Dholakia, "Controlled Rotation of Optically Trapped Microscopic Particles," Science **292**, 912–914 (2001). http://www.sciencemag.org/cgi/content/abstract/292/5518/912.

#101372 - $15.00 USD Received 9 Sep 2008; revised 6 Oct 2008; accepted 7 Oct 2008; published 9 Oct 2008

12. V. Bingelyte, J. Leach , J. Courtial, and M. Padgett, "Optically controlled three-dimensional rotation of microscopic objects," Appl. Phys. Lett. **82**, 829–831 (2003). http://link.aip.org/link/?APPLAB/82/829/1.
13. P. Shaw, D. Agard, Y. Hiraoka, and J. Sedat, "Tilted view reconstruction in optical microscopy. Three-dimensional reconstruction of Drosophila melanogaster embryo nuclei." Biophys. J. **55**, 101–110 (1989). http://www.biophysj.org/cgi/reprint/55/1/101.
14. R. Heintzmann and C. Cremer, "Axial tomographic confocal fluorescence microscopy," J. Microsc. **206**, 7–23 (2002). http://www3.interscience.wiley.com/journal/118942885/abstract.
15. J. Huisken, J. Swoger, F. Del Bene, J. Wittbrodt, and E. Stelzer, "Optical Sectioning Deep Inside Live Embryos by Selective Plane Illumination Microscopy," Science **305**, 1007–1009 (2004). http://www.sciencemag.org/cgi/content/abstract/305/5686/1007.
16. M. Fauver, E. Seibel, J. R. Rahn, M. Meyer, F. Patten, T. Neumann, and A. Nelson, "Three-dimensional imaging of single isolated cell nuclei using optical projection tomography," Opt. Express **13**, 4210–4223 (2005). http://www.opticsexpress.org/abstract.cfm?URI=oe-13-11-4210.
17. J. Swoger, P. Verveer, K. Greger, J. Huisken, and E. H. K. Stelzer, "Multi-view image fusion improves resolution in three-dimensional microscopy," Opt. Express **15**, 8029–8042 (2007). http://www.opticsexpress.org/abstract.cfm?URI=oe-15-13-8029.
18. A. Constable, J. Kim, J. Mervis, F. Zarinetchi, and M. Prentiss, "Demonstration of a fiber-optical light-force trap," Opt. Lett **18**, 1867–1869 (1993). http://ol.osa.org/abstract.cfm?uri=ol-18-21-1867.
19. J. Guck, R. Ananthakrishnan, T. J. Moon, C. C. Cunningham, and J. Käs, "Optical Deformability of Soft Biological Dielectrics," Phys. Rev. Lett. **84**, 5451–5454 (2000). http://prola.aps.org/abstract/PRL/v84/i23/p5451_1.
20. J. Guck, R. Ananthakrishnan, H. Mahmood, T. J. Moon, C. C. Cunningham, and J. Käs, "The optical stretcher: A novel laser tool to micromanipulate cells." Biophys. J. **81**, 767–784 (2001). http://www.biophysj.org/cgi/content/full/81/2/767.
21. D. Gloge, "Weakly guiding fibers," Appl. Opt **10**, 2252–2258 (1971). http://oe.osa.org/ViewMedia.cfm?id=73014&seq=0.
22. D. Gloge, "Dispersion in weakly guiding fibers," Appl. Opt **10**, 2442 (1971). http://ao.osa.org/ViewMedia.cfm?id=72974&seq=0.
23. A. Safaai-Jazi and J. McKeeman, "Synthesis of intensity patterns in few-mode optical fibers," J. Lightwave Technol. **9**, 1047–1052 (1991). http://ieeexplore.ieee.org/xpls/abs_all.jsp?arnumber=85799.
24. S. C. Grover, A. G. Skirtach, R. C. Gauthier, and C. P. Grover, "Automated single-cell sorting system based on optical trapping." J. Biomed. Opt. **6**, 14–22 (2001). http://dx.doi.org/10.1117/1.1333676.
25. K. Franze, J. Grosche, S. N. Skatchkov, S. Schinkinger, C. Foja, D. Schild, O. Uckermann, K. Travis, A. Reichenbach, and J. Guck, "Muller cells are living optical fibers in the vertebrate retina." Proc. Natl. Acad. Sci. USA **104**, 8287–8292 (2007). http://dx.doi.org/10.1073/pnas.0611180104.
26. A. Brunsting and P. F. Mullaney, "Differential light scattering from spherical mammalian cells." Biophys. J. **14**, 439–453 (1974).
27. R. Drezek, M. Guillaud, T. Collier, I. Boiko, A. Malpica, C. Macaulay, M. Follen, and R. Richards-Kortum, "Light scattering from cervical cells throughout neoplastic progression: influence of nuclear morphology, DNA content, and chromatin texture." J. Biomed. Opt. **8**, 7–16 (2003). http://dx.doi.org/10.1117/1.1528950.
28. F. Charriere, N. Pavillon, T. Colomb, C. Depeursinge, T. J. Heger, E. A. D. Mitchell, P. Marquet, and B. Rappaz, "Living specimen tomography by digital holographic microscopy: morphometry of testate amoeba," Opt. Express **14**, 7005–7013 (2006). http://www.opticsexpress.org/abstract.cfm?URI=oe-14-16-7005.
29. O. Renaud, J. Vina, Y. Yu, C. Machu, A. Trouve, H. Van der Voort, B. Chalmond, and S. Shorte, "High-resolution 3-D imaging of living cells in suspension using confocal axial tomography." Biotechnol. J. **3**, 53–62 (2008). http://dx.doi.org/10.1002/biot.200700188.
30. E. R. Dufresne, G. C. Spalding, M. T. Dearing, S. A. Sheets, and D. G. Grier, "Computer-generated holographic optical tweezer arrays," Rev. Sci. Inst. **72**, 1810–1816 (2001).
31. G. Whyte, G. Gibson, J. Leach, M. Padgett, D. Robert, and M. Miles, "An optical trapped microhand for manipulating micron-sized objects," Opt. Express **14**, 12,497–12,502 (2006). http://www.opticsexpress.org/abstract.cfm?URI=oe-14-25-12497.
32. K. König, H. Liang, M. W. Berns, and B. J. Tromberg, "Cell damage in near-infrared multimode optical traps as a result of multiphoton absorption," Opt. Lett. **21**, 1090 (1996). http://ol.osa.org/abstract.cfm?URI=ol-21-14-1090.
33. M. Kreysing, J. Guck, and J. Käs, "Device and method for contactless manipulation and alignment of sample particles in a measurement volume with the aid of an inhomogeneous electrical alternating field." European patent, EP1935498A1 (2007).

#101372 - $15.00 USD Received 9 Sep 2008; revised 6 Oct 2008; accepted 7 Oct 2008; published 9 Oct 2008

1. Introduction

Since Ashkin introduced optical traps in the 1970s [1] they have become versatile tools for the micromanipulation of biological objects. They are commonly used to hold, interactively move, stretch and sort cells [2, 3]. Of particular interest for microscopy, however, is the further improvement of the rotational control of biological samples. Two mechanisms have been demonstrated for the in-plane optical rotation of trapped particles using modified single-beam gradient traps — commonly referred to as optical tweezers. First, laser beams carrying net angular momentum, which can either be spin [4, 5] or orbital angular momentum [6, 7], can be used to induce a continuous spinning of trapped samples. While this can potentially be used for the operation of optically driven micromachines, the stable orientation of particles in a particular orientation, as required by microscopy, is only possible with a complicated closed-loop feedback mechanism. Another approach rotates the sample together with a trapping beam of reduced symmetry. Such rotation has been realized using optical tweezers modified by the use of higher order cavity modes [8], cylindrical lenses [9], rectangular apertures [10], and spiral interference patterns [11]. In addtion, the creation of multiple traps by means of holographic optics has been shown to allow for the rotation of micro bead clusters around arbitrary axis [12].

Although this demonstrates the physical principles of optical rotation, the manipulation of objects with optical tweezers is inevitably coupled to the imaging optics of the microscope and generally limited to objects smaller than a few microns. Furthermore, feedback independent solutions to orient arbitrarily shaped particles, such as cells, have so far been restricted to a rotation around an axis parallel to the optical axis of the microscope and are therefore of limited use for microscopy itself. In particular, tomographic approaches to isotropic microscopy [13–17], which rely on image acquisition from different sides, have so far been unable to benefit from optical rotation.

In this paper we report on a sensible alternative strategy using a dual-beam fiber trap with one non-rotationally symmetric trapping beam. The asymetric beam results from the excitation of higher order modes in a dual-mode optical fiber. Trapped cells, which generally have either a shape- or optical anisotropy, follow the rotation of the beam asymmetry. They can be oriented at arbitrary angles, where the axes of the rotation and the microscope are perpendicular to each other. Since this optical cell rotator (OCR) is decoupled from the imaging optics it can be used on practically any light microscope and promises to find applications in tomographic microscopy techniques aiming at isotropic resolution.

2. Modified dual-beam fiber trap

The basis of OCR is a fiber-based dual-beam laser trap. The original version of this trap was first realized by Ashkin in 1970 [1] (16 years before the introduction of optical tweezers), and technically simplified by Constable in 1993 [18] by employing single-mode optical fibers for beam delivery. This trap makes use of two divergent counter-propagating laser beams and allows stable holding of dielectric particles in tree dimensions. Lateral stability arises from gradient forces centering the specimen on the optical axis. Since axial stabilty is given at the point at which scattering forces of the two beams balance each other, this trapping geometry also works with highly inhomogeneous samples of sizes in excess of $100\mu m$, which would be pushed out of the focus of optical tweezers by the scattering force. If used to deform soft dielectrics this dual-beam trap is referred to as an optical stretcher [19, 20].

The general setup of OCR is shown in Fig. 1. The laser sources used were two Ytterbium-doped non-polarized CW fiber lasers (YLM-2-1064, IPG Photonics, Germany) operating at 1064 nm. The lasers have output fibers that are single-mode at this wavelength (HI 1060, Corning, Germany) and are usually used directly for trapping in fiber-optical traps. Since single mode fibers (SMF) have rotationally symmetric beam profiles these traps do not offer control

#101372 - $15.00 USD Received 9 Sep 2008; revised 6 Oct 2008; accepted 7 Oct 2008; published 9 Oct 2008

over the rotational degree of freedom of a trapped object. Here, we report for the first time on a fiber-based optical trap that allows advanced manipulation of trapped objects by intentionally using more than one transverse optical mode. These were excited by splicing one of the lasers' SMF to a dual-mode fiber (SMF-28 J9, Corning, Germany; cut-off wavelength 1260 nm, core radius 4.2μm) with a defined offset (see Fig. 1(c)) using an arc fusion splicer (S175 V2000, Fitel, Japan).

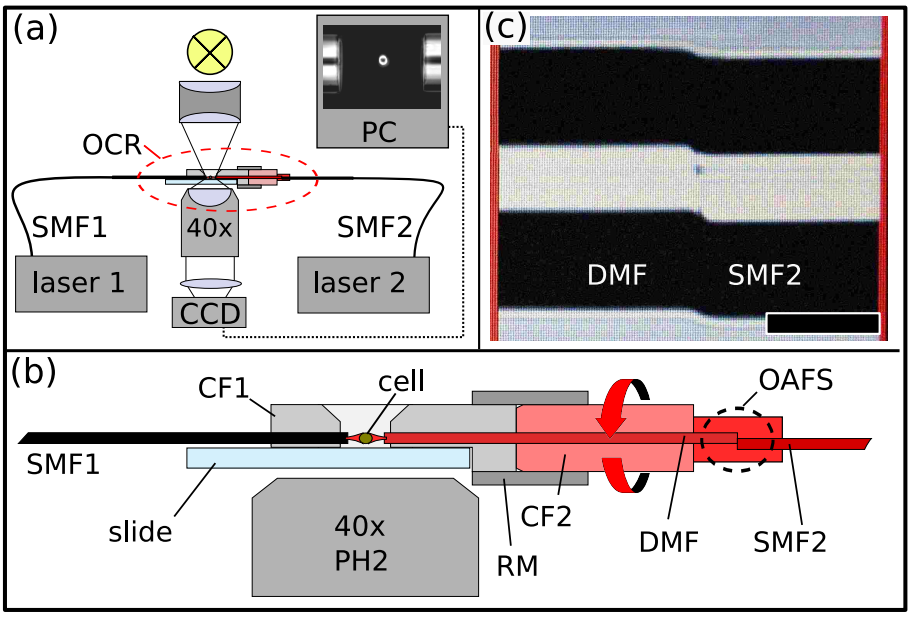

Fig. 1. Schematic of the OCR setup. (a) The OCR is mounted on an inverted microscope. SMF, single-mode fiber. (b) Detailed view of the dashed area indicated in (a). SMF1 is mounted in a ceramic ferrule (CF1). SMF2 is spliced with an offset to a dual-mode fiber (DMF) which is mounted in a second ferrule (CF2). Parts shaded in red form one static unit that can be rotated with respect to the rest of the system in a rotation mount (RM). The trapping and rotation of a cell can be imaged through a glass window (slide). (c) Microsopic image of an offset arc fusion splice (OAFS). Scale bar, 50μm.

3. Dual-mode fiber optics

Coupling of the single-mode beam into the dual-mode fiber was theoretically predicted using scalar wave theory. The propagation of electromagnetic waves in step index optical fibers is usually discussed in terms of the linearly polarized (*LP*) modes introduced by Gloge for the limit of weak light guidance [21]. *LP* modes describe the in-plane electric field distributions of step index fibers as a product of radial and azimuthal functions in polar coordinates, $E = R(r)\Phi(\varphi)$. For the two lowest order modes, E_{LP01} and E_{LP11} are given by

$$E_{LP01} = c_{01} J_0(\kappa_{core}^{01} r) \quad \text{for} \quad r \leq a \tag{1}$$
$$E_{LP01} = c'_{01} K_0(\kappa_{clad}^{01} r) \quad \text{for} \quad r > a$$
$$E_{LP11} = c_{11} J_1(\kappa_{core}^{11} r) cos(\varphi) \quad \text{for} \quad r \leq a \tag{2}$$
$$E_{LP11} = c'_{11} K_1(\kappa_{clad}^{11} r) cos(\varphi) \quad \text{for} \quad r > a \quad .$$

#101372 - $15.00 USD Received 9 Sep 2008; revised 6 Oct 2008; accepted 7 Oct 2008; published 9 Oct 2008

The radial functions $R(r)$ are determined by the oscillatory ordinary Bessel functions of the first kind, $J_l(\kappa_{core}r)$, for the core (radius a) and decaying modified Bessel functions of the second kind, $K_l(\kappa_{clad}r)$, for the cladding. κ_{core} and κ_{clad} are transverse frequencies and the integer l corresponds to the angular quantum number appearing in the azimuthal modulating function $\Phi(\varphi) = cos(l\varphi)$, normalization constants are denoted as c. While the usual boundary conditions determine the transverse frequencies, the number of modes in a step index fiber exclusively depends on the normalized frequency parameter $V = \frac{2\pi}{\lambda} a\,NA$. Here λ is the wavelength and NA is the numerical aperture of the fiber. For $V < 2.405$ only the ground state mode $LP01$ is able to propagate lossfree, for $2.405 \leq V \leq 3.832$ additionally the next higher order mode $LP11$ exists, etc. In time (t) and along the fiber axis (z), this in-plane amplitude distribution is modulated by the ususal phase factor $exp(i(\beta z - \omega t))$, where β is the projection of the wave vector onto the optical axis, and ω stands for the wave's angular frequency.

For our setup fibers with $V = 2.09$ (SMF) and $V = 3.39$ (DMF) were used. Coupling coefficients between the modes of the two fibers depend on the transverse offset, ρ, and were calculated as discretised overlap integrals of the field amplitudes using Matlab. The resulting coupling efficiencies are plotted as functions of ρ in Fig. 2.

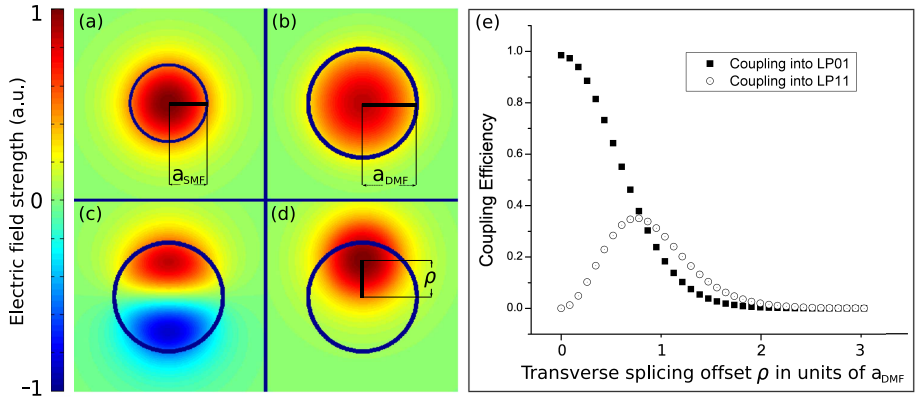

Fig. 2. Field distributions and coupling efficiencies. (a) $LP01$ electric field distribution in SMF. Black circle indicates core boundary. (b) $LP01$ and (c) $LP11$ electric field distributions in fiber with larger core (DMF). (d) Coupling of SMF field distribution, offset by ρ, into DMF. (e) Calculated efficiencies for the coupling from SMF field distribution to the two DMF modes as a function of the transverse offset ρ.

Based on the calculated coupling efficiencies (see Fig. 2(e)) the two fibers were spliced together statically with a transverse offset of $3.2\,\mu m$. This offset value combines strong coupling into the symmetry breaking $LP11$ mode with reasonable overall efficiency. For a step index DMF the intensity distribution at the fiber end is given by the coherent superposition of the two individual modes,

$$I = (E_{LP01} + E_{LP11})^2 = E_{LP01}^2 + E_{LP11}^2 + 2E_{LP01}E_{LP01}cos(\Delta\beta L), \tag{3}$$

where L is the length of the DMF. $\Delta\beta$ is the difference between the propagtion constants,

$$\Delta\beta = \beta_{LP01} - \beta_{LP11}, \tag{4}$$

which underlie a modal phase velocity dispersion [22]. Thus, the intensity pattern at the fiber output varies periodically with increasing fiber length [23]. During one periode each lobe of

#101372 - $15.00 USD Received 9 Sep 2008; revised 6 Oct 2008; accepted 7 Oct 2008; published 9 Oct 2008

the $LP11$ mode goes through constructive and destructive interference with the $LP01$ mode. In order to balance the resulting lobes of the intensity profile, the total phase between the modes at the fiber end needs to be $\frac{\pi}{2} mod(\pi)$. The beating length of the specified DMF was calculated as $\Delta L = \frac{2\pi}{\Delta\beta} \approx 380\,\mu m$. This comfortably allowed to shorten the fiber to the appropriate length using standard fiber polishing equipment (Thorlabs, Germany). During this process the beam profile was repeatedly imaged in a plane approximately $100\mu m$ away from the fiber end face, which coincides with the typical distance between trapped specimen and the fiber end in our experiment. The result of the fiber-based beam shaping is compared with the theoretical prediction in Fig. 3. It should be noted that the phenomenon of modal beating is less pronounced when using lasers with short coherence length or long fibers.

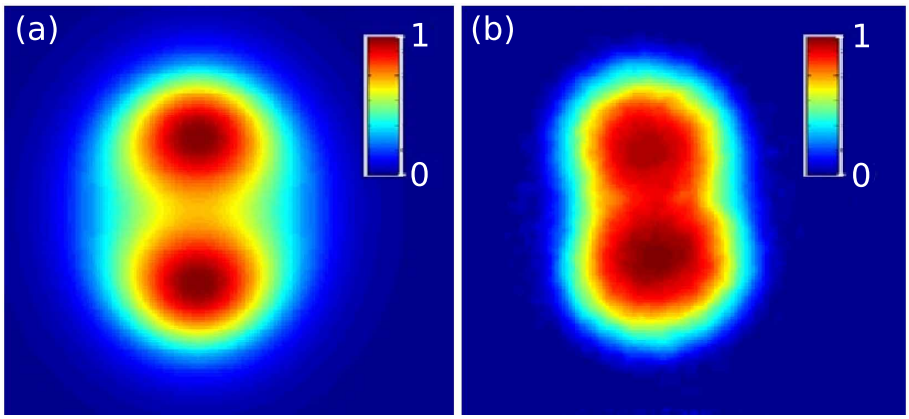

Fig. 3. (a) Calculated and (b) measured beam intensity profile of a DMF excited at $3.2\mu m$ offset.

4. Experiments

Since the orientation of the dual-mode beam profile was determined by the static fiber splice, the rotation of this beam profile had to be achieved by the rotation of the fiber carrying it. Therefore, the two fiber ends were aligned using a specially designed ceramic mounting made from standard FC connector ferrules for fibers with 125 μm outer diameter (Thorlabs, Germany) (see Fig. 1(b)). Accuracy of the rotation of the DMF was assured by a ceramic sleeve bearing, functioning as rotation mount. The maximum torsion of the DMF in the stationary ceramic mounting was measured to be less than 1 degree. To gain optical access to the fiber channel a hole was drilled perpendicular to the channel. In this region the cleaved fiber ends were facing each other with a distance of approximatly 200 μm, forming the trap.

Human red bood cells (RBC), cells from a human leukemia cell line (HL60), and cell clusters of a breast epithelial cancer cell line (MCF-7) were used as specimens. RBCs were prepared by diluting $1\mu l$ of fresh blood from a healthy male donor in $10ml$ isotonic phosphate buffered saline (PBS) solution containing 1 ppt EDTA to avoid blood coagulation. HL60 cells (DMSZ, Germany) were cultured in RPMI 1640 medium containing 10 % heat inactivated fetal bovine serum, $0.3g/l$ L-glutamine, and 1 % penicillin/streptomycin at 37 °C and 5% CO_2. Cells were passaged every 2-3 days and diluted to concentrations of approximately $10^5 ml^{-1}$ for experimental use. Chemicals were obtained from Sigma (Germany). MCF-7 cells (ATCC, USA) were cultured in $75cm^2$ culture flasks using Eagle's minimum essential medium (MEM) supplemented with 10% fetal bovine serum, $0.29g/l$ L-glutamine, 1% penicillin/streptomycin, $0.01mg/ml$ bovine insulin, $0.11mg/ml$ sodium pyruvate and incubated at 37 °C with $5\%CO_2$.

#101372 - $15.00 USD Received 9 Sep 2008; revised 6 Oct 2008; accepted 7 Oct 2008; published 9 Oct 2008

Cells were passaged every 2-3 days and prior to experimental use detached with a 0.05% Trypsin-EDTA solution and resuspended in culture medium at $5 \times 10^5\ ml^{-1}$. These chemicals were obtained from PAA (Austria).

After cleaning the fiber ends with a cleaning agent, the setup was washed with cell culture medium several times. Approximately $500\mu l$ cell suspension was added and exchanged every 5 – 10 minutes in order to keep osmolarity constant. The lasers were operated at output powers between 30 and 150 mW CW per fiber. Cells were trapped randomly from a flow in the medium induced by a micropipette. Some cells and clusters were also trapped inside a square glass capillary. Once a cell or cell cluster reached a stable position and orientation, the dual-mode beam was rotated to induce the rotation of the cell. This rotation was carried out manually by turning the DMF by 5 – 180 degrees with frequencies ranging approximately from 0.05 to 0.5 Hz.

5. Results and discussion

We observed both the stable trapping of cells in three dimensions as well as their successful optically induced rotation. Typical time series of the rotation of RBCs, HL60 cells, and MCF-7 cell clusters are shown in Fig. 4 – 6 . Dealing with real objects that are neither perfectly spherical nor isotropic it has been noted that cells in dual-beam laser traps always align their main anisotropy with the optical axis of the setup, which minimizes the free energy of the system [24, 25]. Any secondary anisotropy should then be oriented in the direction of the asymmetric beam profile introduced by the *LP*11 mode from the DMF. As expected, RCBs were found to align well with the asymmetric intensity profile because of their very asymmetric, biconcave disk-like shape. A rotation of the beam asymmetry with the fiber then causes the RBCs to follow. Their asymmetric shape also makes this rotation easy to observe (Fig. 4).

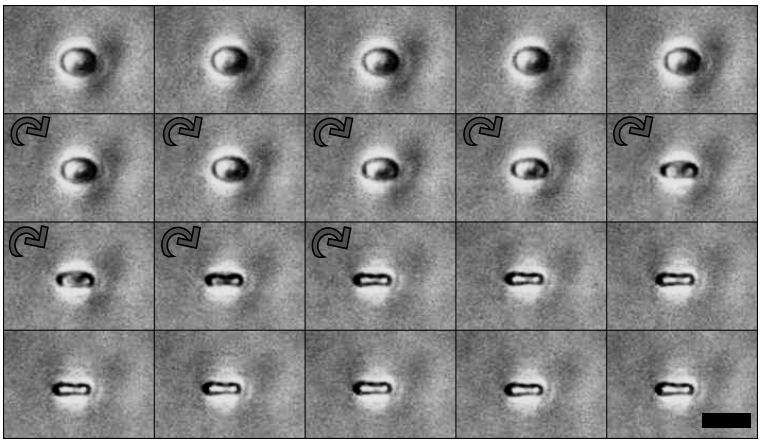

Fig. 4. Phase contrast images of the optical rotation of a red blood cell in time steps of 200 ms. Images obtained while the dual-mode beam profile was turned by 90 degrees are marked. Scale bar, $10\,\mu m$ (Media 1).

Even if the cells have no strong shape anisotropy, as in the case of the largely spherical HL60 cells, the remaining optical anisotropy of the cells is sufficient to orient the cells with the intensity profile. Such an anisotropy is caused by the position and shape of the nucleus, which generally has a higher refractive index than the cytoplasm [26, 27], and a heterogeneous distribution of other internal organelles. The rotation of the HL60 cells can still be followed by tracking the position of characteristic spots on the cell surface (Fig. 5). Also randomly

#101372 - $15.00 USD Received 9 Sep 2008; revised 6 Oct 2008; accepted 7 Oct 2008; published 9 Oct 2008

assembled clusters of MCF-7 cells could be rotated in a controlled way (Fig. 6). For all cell types we observed the angles of rotation of fiber and object to match within an uncertaincy range of a few degrees.

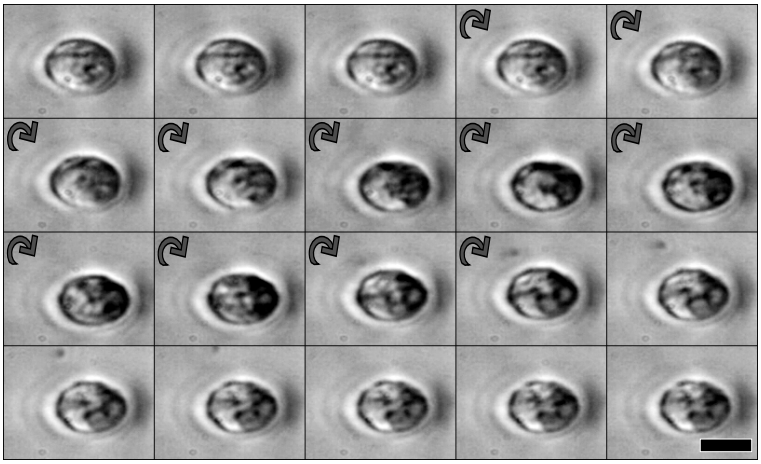

Fig. 5. Phase contrast images of the optical rotation of an HL60 cell in time steps of 320 ms. Images obtained during the rotation of the beam profile are marked. Scale bar, 10 μm (Media 2).

For most of the results shown, the hydrodynamic coupling between the rotating fiber end and the cell could in principle be an alternative explanation of the cell rotation. However, when the laser power was reduced, the cells followed the rotation of the DMF with noticeable delay. The laser power should have no effect on the rotation if it was due to hydrodynamics, which shows that the cells indeed rotate with the potential of the laser beam. Furthermore, small clusters of cells were successfully rotated inside a glas capillary of square cross section placed between the fiber ends (Fig. 6), which shielded the cells from any hydrodynamic coupling.

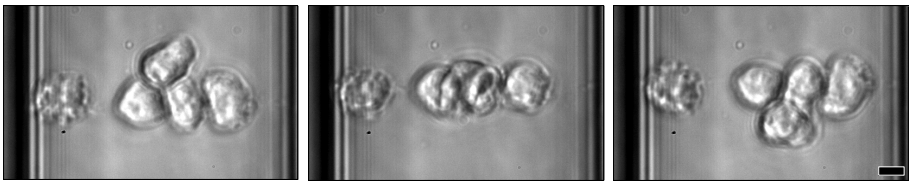

Fig. 6. Optical rotation of a small MCF-7 cell custer inside a microcapillary with rectangular cross section. Scale bar, 10 μm.

Maximum rotational frequencies reached were approximately 0.5 Hz for RBCs at 100 mW and 0.2 Hz for HL60 cells at 150 mW laser power per fiber. This frequency can probably still be increased by using even higher-order fiber modes and the simultaneous rotation of asymmetric beams from both sides. While the lateral displacement of the cells during rotation was generally small, a longitudinal movement (on the beam axis) ranging from 1 to 15 μm was typically observed. The lateral instability was caused by mechanical instabilities in the setup tending to induce significant flow speeds in the medium. The longitudinal movement was clearly induced by the jittering of the turning fiber along its axis. These aspects can be improved in future setups by increased mechanical stability and by avoiding the rotation of the DMF fiber. It is conceivable that the asymmetric beam profile could be rotated through a stationary fiber by

#101372 - $15.00 USD Received 9 Sep 2008; revised 6 Oct 2008; accepted 7 Oct 2008; published 9 Oct 2008

exciting higher-order modes from free space laser beams passing appropriate rotatable phase objects or adaptive optics such as spatial light modulators.

With increased stability, OCR presents a sensible alternative to mechanically rotating biological specimens, embedded in index matching fluid in a microcapillary or held by a micropipette [16, 28]. At the same time OCR offers the advantages of simplicity in setup and control, the ability to rapidly handle many cells in a short amount of time, and reduced artifacts caused by non-physiological conditions. The last aspect is also true in comparison to rotating cells by dielectrophoresis [29]. The main limitations of dielectrophoresis, absent in OCR, are the uncertain viability of sensitive cells due to conductive heating or the requirement of specific media, which might be incompatible with the biology of the cells of interest.

Apart from using a dual-beam trap as described here, an optical rotation of dielectric samples perpendicular to the optical axis of a microscope could also be achieved with holographic optical tweezers (HOTs) [30]. HOTs allow the simultaneous control of multiple foci in 3D for optical tweezing [31]. Trapping and moving three beads attached to a cell as handles in an appropriate sequence would allow a similar controlled rotation as with the OCR. However, beads would likely always be required because otherwise the trapping points and consequently the axis of rotation are not well defined. In addition to the intrinsic axis of rotation achieved without any feedback mechanisms, OCR has the additional advantage over HOTs that, due to the non-focused beams, the intensity on the rotated cell is low, which reduces the risk of photodamage by nonlinear processes [32].

6. Conclusion and outlook

With OCR we present a novel type of optical trap for the controlled rotation of anisotropic dielectric objects, such as cells, with significant advantages over existing techniques. OCR operates fully decoupled from imaging optics and can be used as modular add-on to any light microscope. Using OCR, we have demonstrated that individual human blood cells and cell clusters can be held stably with a well defined orientation and rotated perpendicular to the optical axis of a light microscope using low laser powers. This ability to orient cells stably in three dimensions without exposing them to any mechanical contact should find significant use in biological and medical research. In particular there is big potential in combining OCR with novel imaging techniques that provide isotropic resolution by tomographic reconstrution of samples imaged under multiple angles. To our knowledge this also introduces the use of few-mode fiber optics to the field of optical trapping and opens the possibilty to realize non-trivial trapping geometries based on fiber optics.

Acknowledgments

The authors acknowledge support by the project OSDA, which was funded by the Free State of Thuringia (Germany) and co-financed by the European Regional Development Fund (EFRE). This work led to the application for a European patent [33].

#101372 - $15.00 USD Received 9 Sep 2008; revised 6 Oct 2008; accepted 7 Oct 2008; published 9 Oct 2008